Journal of Catalysis 268 (2009) 79–88

Contents lists available at ScienceDirect

Journal of Catalysis

journal homepage: www.elsevier.com/locate/jcat

An insight into the Meerwein–Ponndorf–Verley reduction of α,β-unsaturated carbonyl compounds: Tuning the acid–base properties of modified zirconia catalysts

Francisco J. Urbano *, María A. Aramendía, Alberto Marinas, José M. Marinas

Department of Organic Chemistry, University of Córdoba, Campus de Rabanales, Marie Curie Building (Annex), E-14014 Córdoba, Spain

ARTICLE INFO

Article history:
Received 20 May 2009
Revised 26 August 2009
Accepted 6 September 2009
Available online 9 October 2009

Keywords:
Zirconia catalysts
Zirconia–Boria
Zirconia–alkaline-earth
Surface acidity
Surface basicity
Meerwein–Ponndorf–Verley reduction
Cinnamaldehyde

ABSTRACT

A series of catalysts consisting of ZrO_2 in pure form or modified by doping with boron or an alkaline-earth metal to enhance their acid and basic properties, respectively, were prepared and used in the Meerwein–Ponndorf–Verley reduction of cinnamaldehyde with 2-propanol, where they exhibited moderate activity and a high selectivity (up to 98%) towards cinnamyl alcohol. The catalyst preparation procedure and its modification (*viz.* doping with boron or an alkaline-earth metal) were found to delay crystallization and increase the number of hydroxyl groups present on the catalyst surface, and hence its catalytic activity. The surface acid and basic properties of the catalysts were determined by pyridine and carbon dioxide chemisorption, respectively. The most active sites in the studied reaction are seemingly proton (Bronsted) acid sites of medium–high strength formed by modification of the ZrO_2 with boron; however, the increased activity thus obtained is accompanied by a loss of selectivity towards cinnamyl alcohol. Modifying ZrO_2 with an alkaline-earth metal enhances its basicity, thereby reducing its catalytic activity and increasing its selectivity for the unsaturated alcohol.

1. Introduction

The reduction of carbonyl compounds by hydrogen transfer from an alcohol is known as the "Meerwein–Ponndorf–Verley reaction" or "MPV reaction" in Organic Chemistry. The presence of a C=C double bond conjugated with the C=O group in an α,β-unsaturated carbonyl compound introduces an additional dimension in the process: the chemoselective reduction of the C=O group in the presence of the C=C bond, which leads to the formation of an α,β-unsaturated alcohol. This selective synthesis for primary and secondary alcohols is an important process in pharmaceutical, fragrance and food flavouring industries. Their preparation by catalytic hydrogenation with a metal-supported catalyst is rather difficult owing to the high reactivity of the C=C bond relative to the carbonyl group [1] although some interesting results have been reported [2]. However, the MPV reaction has been successfully used for the selective reduction of the C=O bond in α,β-unsaturated carbonyl compounds to the corresponding unsaturated alcohols.

Traditionally, the MPV reaction has been conducted by using a metal (Al, Zr) alkoxide as catalyst in a homogeneous process. The reaction mechanism involves the formation of a six-membered cyclic intermediate where both reactants coordinate to the same metal site in the alkoxide [3–5]. The past two decades, however, have seen a rise in research aimed at facilitating conduct of the process in a heterogeneous phase on account of the major advantages of operating in this way in large-scale processes [4].

The reduction of α,β-unsaturated carbonyl compounds by hydrogen transfer under heterogeneous catalysis has so far been studied in the presence of a variety of catalysts including magnesium hydroxides [6], magnesium oxides [7–9], hydrous and calcined zirconia [7,10,11] and a wide range of active components supported on zeolitic [3,12], mesoporous [13,14] and various other materials [15].

Although the mechanism behind these heterogeneous hydrogen transfer processes is seemingly quite clear, there remains some uncertainty as to the respective roles of surface acid (Lewis or Bronsted) and/or basic sites in the catalysts. Rather than a unified mechanism, researchers have proposed a number of them dependent on the particular catalyst used in the heterogenous MPV reaction. Thus, the reduction of carbonyl compounds by hydrogen transfer has been hypothesized to occur at Lewis acid sites, basic sites and acid–base pairs [8,16]. In fact, some suitably activated zeolites have proved highly efficient in the hydrogen-transfer reduction of carbonyl compounds, the mechanism behind which, consistent with the decreased activity observed upon addition of pyridine to the reaction medium, appears to involve Lewis acid sites [3]. On the other hand, activity in the MPV reaction in the presence of basic zeolites, magnesium oxides and other, essentially basic catalysts, has been found to decrease upon addition of CO_2 and benzoic acid, which suggests that the process takes place at basic sites [17,18].

* Corresponding author. Fax: +34 957212066.
E-mail address: FJ.Urbano@uco.es (F.J. Urbano).

0021-9517/$ - see front matter © 2009 Elsevier Inc. All rights reserved.
doi:10.1016/j.jcat.2009.09.005

However, a recent study revealed that the catalytic activity in the MPV reaction decreases with increasing calcination temperature (*i.e.* with increasing loss of surface hydroxyl groups) in hydrous zirconia; this underlines the significance of proton (Bronsted) sites in the process [11,10]. In any case, the presence of very strong acid sites appears to reduce the selectivity via side reactions [10,11]. In this respect, surface-modifying MgO with chloroform has been found to seemingly block the Lewis acid sites leading to poisoning of the catalyst and producing acid enough surface OH groups (*viz.* Bronsted acid sites) for the reaction [19–21].

The loss of selectivity by effect of the reduction of the C=C double bond has been ascribed to adsorption of the α,β-unsaturated carbonyl compound via the above-mentioned double bond favoured by the presence of strong Lewis acids [8].

Zirconia has proved a highly effective choice among heterogeneous catalysts used in the MPV reaction [11]. Zirconium oxide is a solid with a high thermal stability and corrosion resistance in addition to a strong amphoteric character [22]. Its textural and acid–base properties depend largely on its synthetic procedure and calcination temperature. Adjusting its acid–base properties is possible by modifying its surface with sulphate ions [23–25], phosphate ions [26] and mixtures of other oxides; this has proved a highly effective method for tailoring the activity of zirconia towards many organic processes. Boron oxide is one of the most widely used compounds for altering the textural and acid–base properties of metal oxides such as Al_2O_3 [27], $AlPO_4$ [28], TiO_2 [29], ZrO_2 [30,31] and MgO [32], which have their acid sites grown at the expense of basic sites. On the other hand, the presence of alkaline-earth metals in metal oxides and mixed oxides has been found to endow the final catalyst with a basic character [33–37].

This piece of research deals with the selective reduction of cinnamaldehyde by hydrogen transfer from 2-propanol in the presence of various solids consisting of ZrO_2 in pure form or modified to alter its acid (ZrO_2–B_2O_3) or basic properties (ZrO_2–alkaline-earth metal). Altering the surface chemical properties of the starting ZrO_2 allowed us to examine the influence of acid (Bronsted *vs.* Lewis) sites and basic sites on activity and selectivity in the selective reduction of α,β-unsaturated carbonyl compounds by hydrogen transfer from 2-propanol.

2. Experimental

2.1. Catalyst synthesis

The catalysts were obtained by thermal treatment of a hydroxygel prepared by alkaline hydrolysis of the corresponding zirconium precursors: zirconyl chloride (Merck) and zirconium propoxide (Fluka); boron (boric acid and trimethylborate from Fluka); and the alkaline-earth metals (magnesium, calcium, strontium and barium carbonates from Merck). The proportions of each other were calculated for an atomic ratio Zr/B = 10 or Zr/alkaline-earth = 13 in the final catalyst.

Gels were obtained by adding 5 M ammonia to a solution of each precursor in 250 mL of milliQ water up to pH 10 under vigorous stirring. The mixture was then refluxed for 24 h, vacuum-filtered and washed with milliQ water to remove all chloride ions as checked with the $AgNO_3$ test. The solid residue was air-dried for 24 h, suspended in isopropanol, rotated for 5 h and the solvent removed by vacuum evaporation at 50 °C. The final texture of solid thus obtained was a fine dust instead of a rock type solid. The resulting hydroxygels were vacuum-calcined at 400 °C for 5 h to obtain the final catalysts.

The name of each catalyst includes the elements forming the solid and information about the zirconium precursor (O for Zr oxychloride and P for Zr propoxide), boron (A for boric acid and T for trimethylborate) or alkaline-earth metal precursor (N for the nitrate).

2.2. Catalyst characterization

Gels were subjected to thermogravimetric and differential thermal analysis on a Setaram Setsys 12 system, using Air at 40 mL/min as carrier gas, α-Al_2O_3 as reference material and a Pt/Pt–Rh(10%) thermocouple. The heating rate was 10 °C/min and the temperature range 30–800 °C. The amount of gel used in each test was *ca.* 17 mg.

The elemental analysis of the catalysts was performed on a Perkin–Elmer ELAN DRC-e ICP-MS instrument following digestion of the samples in a 1:1:1 mixture of HF, HNO_3 and H_2O, and dilution in 3% HNO_3. Calibration samples were prepared from appropriate atomic spectroscopy standards (PE Pure Plus, Perkin–Elmer) in HNO_3 (10 μg/mL of each metal). Calibration curves were constructed over the concentration range 1–100 ppb and the results were included for a blank.

The textural properties of the solids were determined from nitrogen adsorption–desorption isotherms obtained at liquid nitrogen temperature on a Micromeritics ASAP-2010 instrument. All samples were degassed to 0.1 Pa at 110 °C prior to measurement. Surface areas were calculated by using the Brunauer–Emmett–Teller (BET) method [38], while pore size distribution (PSD), mean pore diameter (D_{BJH}) and cumulative pore volume (V_{BJH}) were all determined with the Barrett–Joyner–Halenda (BJH) method [39]; the adsorption branch, the amount of cylindrical pores open on one end only and the adsorbed layer thickness were calculated using the Halsey method.

X-ray diffraction patterns were obtained on a Siemens D5000 diffractometer equipped with a graphite monochromator and using Cu K_α radiation. The 2θ angle was scanned from 5° to 85° with a step size of 0.02°. The average diameter of the zirconia crystallites, d, was calculated from the full width at half maximum (FWHM) of the X-ray reflection at $2\theta = 30.3$ (tetragonal phase), using the Scherrer equation.

FT-Raman spectra were obtained on a Perkin–Elmer 2000 NIR FT-Raman system equipped with a diode-pumped NdYAG laser (9394.69 cm^{-1}) that was operated at 300 mW laser power and a resolution of 4 cm^{-1} throughout the 3500–200 cm^{-1} range in order to gather 64 scans.

Surface acidity in the catalysts was determined from the FT-Raman spectra for chemisorbed pyridine. The most sensitive Raman vibration of pyridine is its symmetric ring breathing (νCCN) (vs, ν_1, A_1), which appears at 991 cm^{-1} in liquid pyridine. The interaction of pyridine with acid sites induces a shift of this band to a higher wavenumber. Therefore, the position of the skeletal vibration band can be used to detect interactions between pyridine and protonic weak acid sites through hydrogen bonds (996–1008 cm^{-1}) or its chemisorption at strong Bronsted (1007–1015 cm^{-1}) and/or Lewis acid sites (1018–1028 cm^{-1}) on a solid surface [40–42].

Chemisorbed pyridine FT-Raman measurements were made in a Ventacon H4 environmental cell coupled to the FT-Raman instrument. A nitrogen stream at 50 mL/min was saturated with pyridine at room temperature and then flowed through a catalytic bed at 50 °C for 1 h. Then, physisorbed pyridine was removed by flowing nitrogen at 40 mL/min until complete disappearance of the peak for physisorbed pyridine at 991 cm^{-1}. Spectra were recorded using a resolution of 4 cm^{-1}, a laser power of 300 mW and 64 accumulations. The spectra obtained after clean-up were subsequently processed with the software PeakFit v. 4.11 in order to determine the components for physisorbed and chemisorbed pyridine in their three variants (hydrogen-bonding interactions, Bronsted sites and Lewis sites).

Catalyst basicity was determined using a pulse method on a Micromeritics TDP/TPR 2900 instrument equipped with a thermal conductivity detector. Carbon dioxide (10% in argon) was employed as the probe molecule. Before titration, the catalyst (50 mg) was cleaned in an Ar stream at 50 ml/min at 400 °C for 30 min. This was followed by cooling to the working temperature (50 °C). The amount of chemisorbed CO_2 was determined by injecting 100-μl CO_2 pulses containing 10% argon until a constant area signalling saturation of the catalyst surface was obtained.

2.3. Catalytic tests

The catalytic hydrogen-transfer reaction was conducted in a two-mouthed flask furnished with a magnetic stirrer and a condenser. An amount of 0.09 mol of isopropyl alcohol was supplied with 0.003 mol of carbonyl compound and the mixture was refluxed with stirring at 1000 rpm. The reaction was started by feeding 0.5 or 1 g of freshly calcined catalyst to the mixture. Several aliquots of the mixture were withdrawn during the course of the reaction for analysis on a Fisons Instruments GC 8000 Series gas chromatograph furnished with a 30 m long, 0.53 mm i.d. Supelcowax-10 semi-capillary column and fitted to a flame ionization detector (FID).

The reaction products obtained for the cinnamaldehyde (UAL) reduction were the cinnamyl alcohol (unsaturated alcohol, UOL), 3-phenylpropanol (saturated alcohol, SOL) and 3-phenylpropanal (saturated aldehyde, SAL). The initial reduction rate of cinnamaldehyde was calculated from the initial slope of the substrate reaction profile at conversions below 10% and expressed in terms of catalyst weight (g) and surface area (m^2). The selectivity towards the unsaturated alcohol at variable conversion levels was calculated from the following expression:

$$S_{UOL} = (\text{mol cinnamyl alcohol/mol cinnamaldehyde converted}) \times 100.$$

3. Results

3.1. Catalytic systems

3.1.1. Thermal analysis and chemical composition of the catalysts

Fig. 1 shows the FT-Raman spectra for the precursor gels of the studied catalysts. As can be seen, all except those for Zr–O and ZrCa–PN exhibited the typical bands for isopropanol incompletely removed during rotaevaporation and drying, and retained in the gels as a result. Such bands included those for the stretching vibration of C–H bonds in saturated chains below 3000 cm^{-1} and chain vibrations for aliphatic compounds at *ca.* 821 cm^{-1}.

On the other hand, by way of example, Fig. 2 shows the TGA–DTA–DTG profiles for the solids Zr–O and Zr–P. As can be seen, they exhibited an endothermic peak centred at *ca.* 115 °C that was assigned to the loss of water and, for the gels containing alkaline-earth metals, also to that of CO_2. In addition, the spectrum for Zr–P exhibited an exothermic peak centred at 287 °C due to the combustion of isopropanol retained in the gel, which, as noted earlier, reflected in the FT-Raman spectra for all gels except Zr–O and ZrCa–PN. Finally, all gels exhibited an exothermic peak centred at *ca.* 440–475 °C for the Zr gels and at 500–600 °C for the Zr solids modified with boron or an alkaline-earth metal. Such a peak, which is known as the "glow exotherm" in the literature, was assigned to crystallization of the gel in the monoclinic or tetragonal system, which resulted in internal structural rearrangement.

The temperature of the "glow exotherm", T_{glow}, depends on the composition of the particular gel as presented in Table 1. Thus, the presence of additives such as boron or an alkaline-earth metal delayed crystallization of the gel and shifted T_{glow} to higher levels: 473 and 442 °C for Zr–O and Zr–P, respectively, and 512, 539, 588 and 598 °C for ZrB–OA, ZrB–OT, ZrB–PA and ZrB–PT, respectively. This was also the case with the gels containing an alkaline-earth metal, which exhibited a markedly higher T_{glow} value than those consisting for pure zirconium oxide: 506 °C for

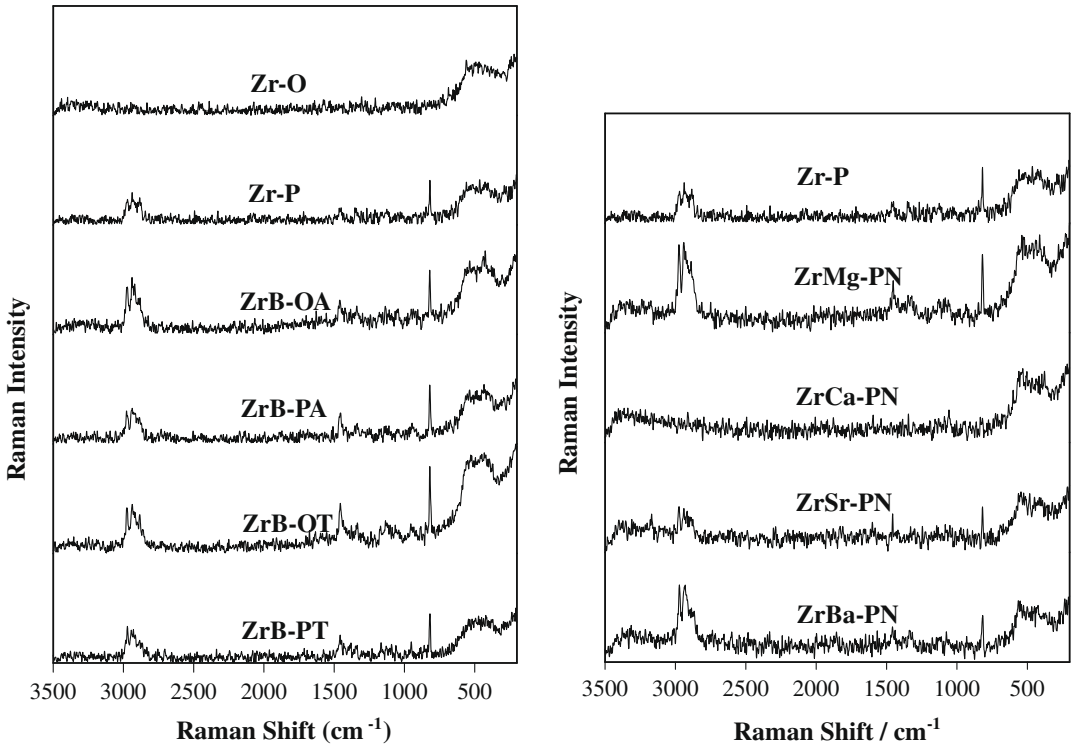

Fig. 1. FT-Raman spectra for the precursor gels of the synthesized catalysts.

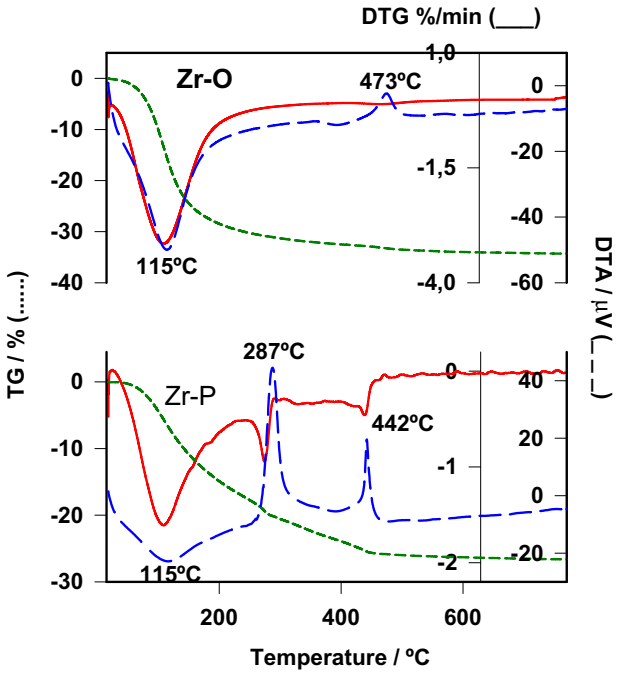

Fig. 2. TGA–DTA–DTG profiles for the precursor gels of the Zr–O and Zr–P catalysts.

ZrMg–PN, 513 °C for ZrCa–PN, 564 °C for ZrSr–PN and 590 °C for ZrBa–PN.

Table 1 also shows the results of the chemical analysis of the studied catalysts. All boron-containing solids exhibited a lower B content than expected. However, the amount of boron contained in the catalysts obtained from zirconium propoxide (about 1 wt% B) was greater than that present in the catalysts prepared from zirconium oxychloride (about 0.4 wt% B). This is consistent with the increased crystallization (glow exotherm, T_{glow}) temperature found in the differential thermal analysis (DTA) of the catalysts ZrB–PA and ZrB–PT relative to ZrB–OA and ZrB–OT, which contained less boron.

The solids containing an alkaline-earth metal exhibited a proportion of Mg slightly higher than its theoretical value. This was not the case with the solids containing Ca, Sr or Ba, which exhibited contents increasingly departing from their theoretical counterparts. This discrepancy can be explained in terms of the solubility products for the corresponding hydroxides, which increase as one moves down the alkaline-earth group. Even though the atomic proportion of Ba was lower than that of Mg, the large difference in atomic weight between the two metals resulted in an increased proportion of Ba in the catalyst relative to Mg; as a result, the crystallization temperature for ZrBa–PN was higher than that for the other catalysts in our series.

3.1.2. Textural and structural characterization

Table 1 also summarizes the specific surface area (S_{BET}, m^2/g) of the catalysts obtained from their nitrogen adsorption–desorption isotherm. Such isotherms for all zirconium oxides studied, both pure and modified, were type IV in the classification of Brunauer et al. [38] and hence typical of mesoporous materials. This indicates that modifying the solids with boron oxide or an alkaline-earth metal introduces no textural changes in the resulting catalyst. As can be seen from the table, solids ZrB–PA and ZrB–PT exhibited a markedly greater surface area than all others while ZrB–OA and Zr–P were the solids having the lowest S_{BET} values.

Fig. 3 shows the XRD patterns for the catalysts. Using the Scherrer equation allowed the average crystallite size for the catalysts exhibiting some crystallinity to be calculated (see Table 1). Both pure zirconium oxides (Zr–O and Zr–P) crystallized in the tetragonal system ($2\theta = 30$) and exhibited no bands for the monoclinic system ($2\theta = 29$ or $2\theta = 30$). Among the boron-containing solids, those obtained from zirconium oxychloride (ZrB–OA and ZrB–OT) crystallized in the tetragonal system ($2\theta = 30$), whereas those prepared from zirconium propoxide (ZrB-PA and ZrB-PT) were amorphous. Finally, the solids containing an alkaline-earth metal were crystalline (tetragonal) in the case of ZrMg–PN and ZrCa–PN and essentially amorphous in the case of ZrSr–PN and, especially, ZrBa–PN. Therefore, crystallinity in the solids decreased in descending order of the elements in group II, from Mg to Ba.

The TGA–DTA–DTG, nitrogen adsorption and XRD results are mutually consistent and facilitate our understanding of the process by which the precursor gel becomes a catalyst with a certain specific surface area and crystallinity. Thus, one can assume that the loss of specific surface area will peak when an amorphous gel crystallizes and rearranges itself internally. Also, the crystallization temperature is governed by the glow exotherm point, T_{glow}, which in turn is influenced by the presence of additives and their proportion in the solid. Thus, an increased amount of additive helps the gel to stabilize and shifts T_{glow} to much higher values than those for the pure zirconium oxide gels (440–470 °C) approaching 600 °C in some cases. In this respect, the results of the chemical analyses indicate that the amount of boron present in the catalysts obtained from zirconium oxychloride is considerably smaller than that present in the solids prepared from zirconium propoxide; this is consistent with the decreased T_{glow} value for the former (512 °C for ZrB–OA and 539 °C for ZrB–OT) relative to ZrB–PA and ZrB–PT (588 and 598 °C, respectively). Although the catalysts containing an alkaline-earth metal were prepared in the same metal/Zr atomic ratio, the increase in atomic weight as one descends in their periodic group led to the percent weights in the final solids increase from Mg to Ba; this resulted in a gradual shift in the solid crystallization temperature that reflected in T_{glow} (506 °C for ZrMg–PN, 513 °C for ZrCa–PN, 564 °C for ZrSr–PN and 590 °C for ZrBa–PN).

Since all catalysts were vacuum-calcined at 400 °C for 5 h, we can assume that the gels crystallizing to some extent were those

Table 1
Thermal properties of the precursor gels, and chemical, textural and structural properties of the final catalysts.

Catalyst	T_{glow} (°C)[a]	Theoretical composition % w/w	ICP composition% w/w	S_{BET} ($m^2\ g^{-1}$)	Crystallite diameter from XRD (nm)	Crystalline phase
Zr–O	473			172	11	Tetragonal
Zr–P	442			140	11	Tetragonal
ZrB–OA	512	0.85 (B)	0.39 (B)	135	13	Tetragonal
ZrB–OT	539	0.85 (B)	0.37 (B)	170	10	Tetragonal
ZrB–PA	588	1.20 (B)	1.02 (B)	247	–	Amorphous
ZrB–PT	598	1.20 (B)	1.05 (B)	240	–	Amorphous
ZrMg–PN	506	1.45 (Mg)	1.80 (Mg)	172	12	Tetragonal
ZrCa–PN	513	2.36 (Ca)	2.22 (Ca)	154	12	Tetragonal
ZrSr–PN	564	5.00 (Sr)	3.70 (Sr)	191	–	Amorphous
ZrBa–PN	590	7.66 (Ba)	4.70 (Ba)	209	–	Amorphous

[a] Temperature of the "glow exotherm" obtained from the TGA–DTA–DTG analysis of the precursor gels of the catalysts.

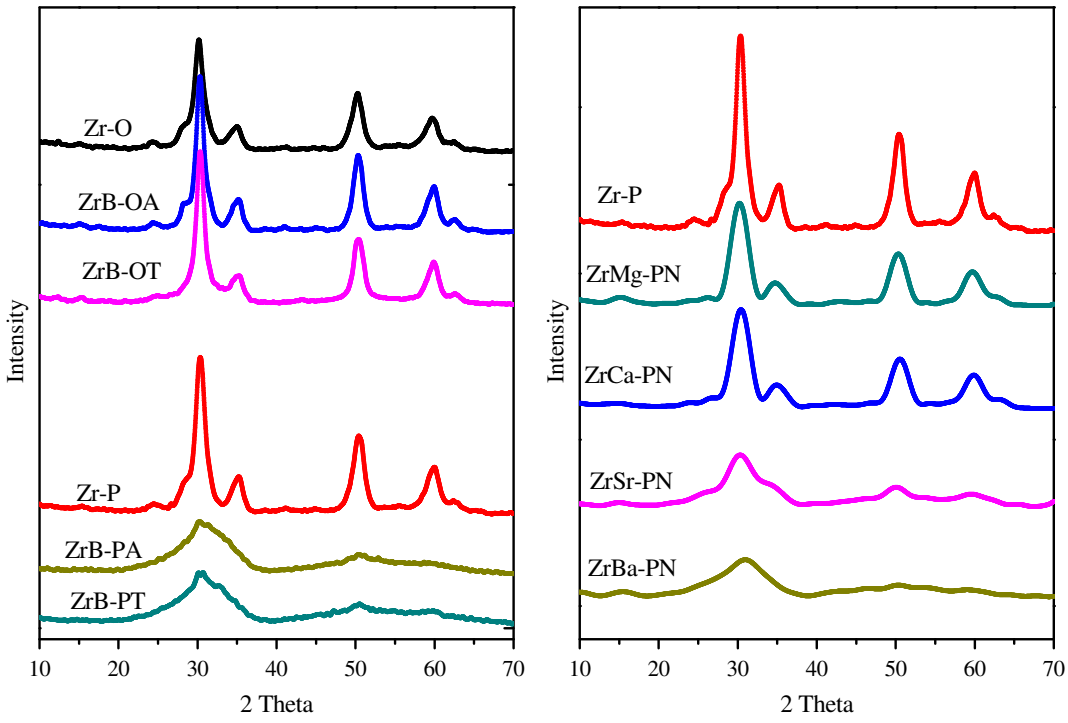

Fig. 3. Powder X-ray diffraction patterns of the synthesized catalysts.

with the lowest T_{glow} values – near the calcination temperature – and thus leading to catalysts with a relatively low specific surface area; in fact, the solids ZrB–OA, ZrB–OT, ZrMg–PN and ZrCa–PN all had $S_{BET} < 200\ m^2/g$. On the other hand, the gels with a high T_{glow} value failed to crystallize during calcination and led to materials with an increased specific surface area; in fact, ZrB–PA, ZrB–PT and ZrBa–PN had $S_{BET} > 200\ m^2/g$. Therefore, the specific surface area of the final catalysts was fairly in good correlation with the crystallization temperature, T_{glow}, of the starting gels (see Fig. 4).

3.1.3. Surface acid–base properties

There have been few attempts in determining surface acidity in solid catalysts by Raman spectroscopy ever since the pioneering work of Hendra and co-workers in this area was published [43,44]. However, the increasing availability of FT-Raman instruments and the development of effective techniques to avoid previously serious fluorescence-related problems have facilitated the use of this technique for the surface chemical characterization of catalytic solids by adsorption of probe molecules such as pyridine [40–42,45].

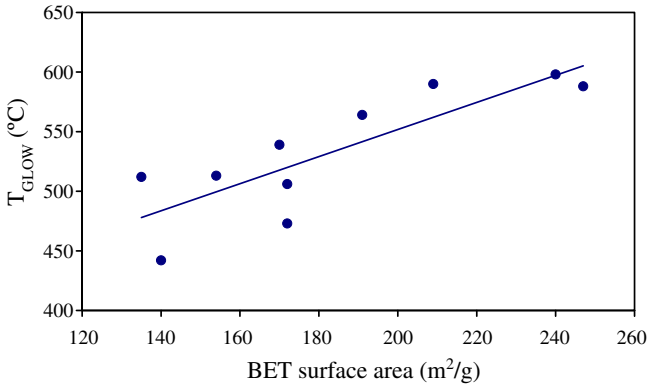

Fig. 4. Crystallization temperature (T_{glow}) obtained from TGA–DTA–DTG experiments and specific surface area (S_{BET}) of the catalysts studied.

In this work, we determined the surface acid properties of the catalysts by using FT-Raman spectroscopy to measure pyridine chemisorption in the solids. The ring-breathing vibration band (νCCN, ν_1) for physisorbed pyridine at 993 cm^{-1} in the resulting spectra increased gradually until each catalyst became saturated with the probe. Evacuation strongly decreased the band, which disappeared altogether or was reduced to small peaks or shoulders of the bands associated to the interaction of pyridine with acid sites in the catalyst. The interaction reflected in a band for pyridine hydrogen-bonded to proton sites (very weak interaction), one for pyridinium ion formed by complete transfer of a proton from a Bronsted acid site to a pyridine molecule (very strong interaction) and one for the formation of a charge-transfer complex between the pyridine molecule and a Lewis acid site (very strong interaction). Fig. 5 shows, as an example, the deconvoluted FT-Raman spectra obtained following pyridine chemisorption on the Zr–P catalyst. The results for all catalysts are presented in Fig. 6, which includes the proportions of acid sites as calculated from the pyridine adsorption data for all catalysts and, in numerical form, in Table 2.

The catalysts consisting of pure zirconium oxide (Zr–O and Zr–P) exhibited essentially Bronsted acid sites in addition to a small proportion (*ca.* 3%) of Lewis acid sites. Moreover, those Bronsted acid sites interacting only weakly (by hydrogen bonding) with pyridine, accounted for 20–30% of all, whereas those of the same type involved in a complete proton transfer prevailed in both catalysts (Zr–O and Zr–P), where they accounted for 77% and 65% of sites, respectively.

The catalysts modified with boron exhibited an increased amount of Lewis acid sites, which, however, only exceeded a proportion of 10% of all acid sites in ZrB–PA, with 22%. The increase in Lewis acid sites occurred at the expense of Bronsted acid sites, the proportion of which in ZrB–PA was reduced to 48%. On the other hand, the proportions of weak (hydrogen-bonded) and Bronsted acid sites remained at the same levels as in the pure zirconium oxides. In any case, the catalysts consisting of pure zirconium oxide

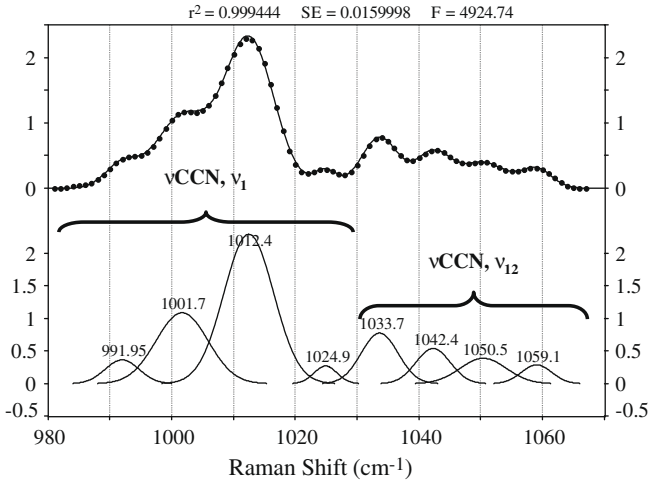

Fig. 5. FT-Raman spectrum of pyridine chemisorbed over the Zr–P catalyst. Deconvolution of the ring-breathing vibration peak (νCCN, ν_1 mode) according to physisorbed pyridine (991 cm^{-1}), hydrogen-bonded pyridine (1002 cm^{-1}), pyridinium ion (Bronsted interacting pyridine, 1012 cm^{-1}) and Lewis adduct of pyridine (1025 cm^{-1}).

and those modified with boron contained mostly strong acid (Bronsted and Lewis) sites, in proportions up to 85%, and relatively few (32%) weak (hydrogen-bonded) acid sites.

As with the boron-modified catalysts, the catalysts containing an alkaline-earth metal contained the three above-described types of acid sites; however, their most common sites were the weakest ones (*viz.* those hydrogen bonded to pyridine), in proportions of 63–85%. Overall, the increase in this type of site occurred at the expense of Bronsted sites; as a result, these catalysts are less acidic than those consisting of pure or boron-modified zirconium. However, the solid ZrMg–PN departed from this trend as it contained more Bronsted acid sites (59%) than weaker acid sites (39%), which made it the most acid catalyst among the zirconium oxides doped with an alkaline-earth metal.

Fig. 6 illustrates the acidity of the studied catalysts ranked according to acid site density (Py/m^2). Overall, the solids Zr–P and ZrMg–PN were those adsorbing the greatest amounts of pyridine, followed by the zirconium oxides doped with an alkaline-earth metal; the latter, however, contained a high proportion of weak acid sites. Then came the catalysts modified with boron oxide, which were the least acidic overall, but were capable of protonating pyridine via their Bronsted acid sites. In addition, ZrB–PA was the only solid interacting to a substantial extent with pyridine via its Lewis acid sites, which accounted for more than 20% of all acid sites.

Table 2
Surface acid–base properties of ZrO_2-based catalysts. Acidity obtained from pyridine chemisorption (FT-Raman detection); Basicity from carbon dioxide chemisorption.

Catalyst	Acidity[a]		Basicity	
	PY total area	PY area/m^2	μmol/CO_2/g	μmol CO_2/m^2
Zr–O	28.0	0.163	54.18	0.31
Zr–P	33.2	0.237	61.89	0.44
ZrB–PT	28.7	0.120	1.72	0.01
ZrB–PA	36.2	0.147	5.39	0.02
ZrB–OT	28.2	0.166	15.04	0.08
ZrB–OA	23.3	0.173	2.80	0.02
ZrSr–PN	40.1	0.210	118.5	0.62
ZrMg–PN	39.0	0.227	78.76	0.46
ZrBa–PN	42.7	0.204	96.7	0.46
ZrCa–PN	32.1	0.209	107.5	0.69

[a] From the FT-Raman spectra of the ring-breathing vibration νCCN (ν_1 mode) of chemisorbed pyridine in different environments.

As far as the surface basic properties are concerned, Table 2 also shows the results of the CO_2 pulse chemisorption tests used to determine the basic properties of each catalyst. As expected, doping with an alkaline-earth metal resulted in markedly increased basicity in the solids. Also, the boron-modified solids were much less basic than the pure zirconium oxides. Thus, the basicity, in μmol CO_2/m^2, was highest for ZrCa–PN and ZrSr–PN, which were the solids exhibiting the highest density of basic sites, followed by ZrBa–PN and ZrMg–PN. The pure zirconium oxides fell in between the previous two couples and the boron-modified oxides were much less basic than all others.

3.2. Cinnamaldehyde reduction

The above-described solids were tested as catalysts for the reduction of cinnamaldehyde by hydrogen transfer from 2-propanol (*i.e.* the Meerwein–Ponndorf–Verley reaction). Fig. 7 shows

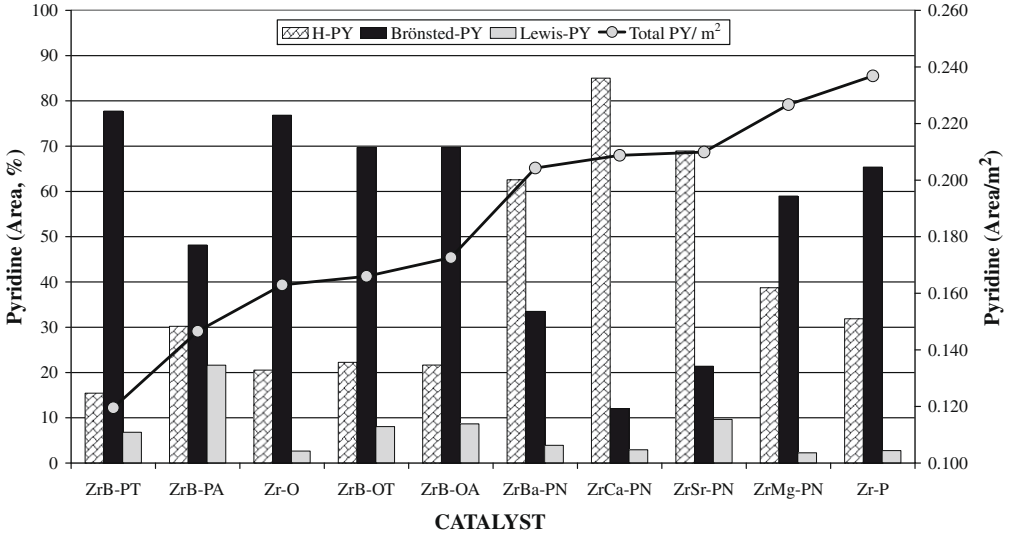

Fig. 6. Surface acidity from pyridine chemisorption (FT-Raman detection) of the catalysts ranked according to its acid sites density (Total Py/m^2). Contribution of each type of pyridine-acid site interaction as obtained from the deconvoluted FT-Raman spectra. H-PY, hydrogen-bonded Pyridine; Bronsted-PY, pyridinium ion; Lewis-PY, Pyridine coordinated to Lewis sites.

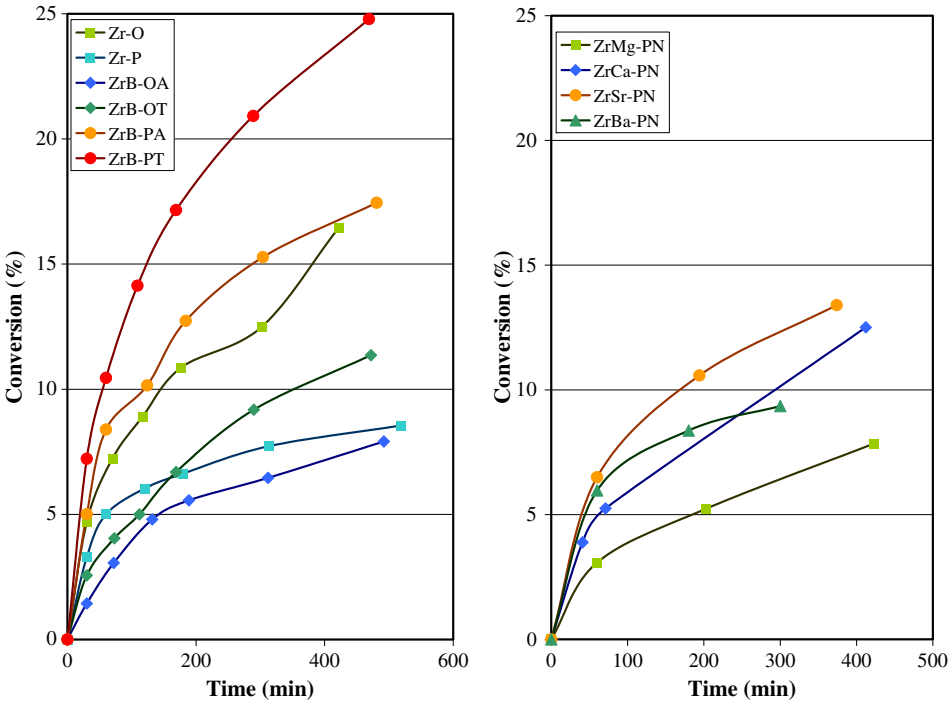

Fig. 7. Reaction profiles (conversion, %) obtained for the Meerwein–Ponndorf–Verley reduction of cinnamaldehyde with 2-propanol over the prepared catalysts.

the respective reaction profiles. As can be seen, all solids had a similar profile and exhibited total conversion values at 8 h ranging from 8% for ZrB–OA to 25% for ZrB–PT.

The reaction products obtained were the unsaturated alcohol (cinnamyl alcohol), saturated alcohol (3-phenylpropanol) and saturated aldehyde (3-phenylpropanal) in all cases. Although the catalysts had acid and/or basic properties, no by-product resulting from the potential dehydration of the unsaturated alcohol at acid sites [18] or condensation at basic sites [8] was detected. In this respect, Chuah et al. found calcining ZrO_2 above 400 °C to reduce the formation of by-products through reversible removal of hydroxyl (acid) groups from the catalyst surface. On the other hand, lower calcination temperatures (in the region of 200 °C) are known to remove no surface hydroxyl groups and to cause the formation of by-products resulting from etherification between cinnamyl alcohol and 2-propanol [11]. The absence of by-products under our reaction conditions (*viz.* 5 h in the presence of catalysts calcined at 400 °C) is consistent with the previous findings.

Table 3 shows the initial reduction rate of cinnamaldehyde, conversion and selectivity obtained with the different catalysts. Based on these results, the catalysts differed markedly in activity. Thus, the solid ZrB-PT was 10 times more active per square metre than were ZrMg–PN and ZrBa-PN; also its initial reduction rate was twice that obtained with the catalysts immediately following it in activity (Zr–O and ZrB–PA).

3.2.1. Selectivity towards the unsaturated alcohol

Table 3 shows the selectivity towards cinnamyl alcohol obtained when the reaction was stopped. As can be seen, all solids exhibited a high selectivity (more than 85% in all instances for cinnamyl alcohol in the reduction of cinnamaldehyde with 2-propanol). However, the catalysts modified with an alkaline-earth metal were especially selective, with values invariably exceeding 97%. These solids were in fact the solids with the highest surface basicity and the least active in the process. On the other end, the solids consisting of pure zirconium oxide (Zr–O and Zr–P) exhibited selectivity levels around 88% towards the unsaturated alcohol. In between these two extremes were the solids in the ZrB series, with highly variable selectivity levels ranging from 88% for ZrB–PA to 97% for ZrB–OT. Irrespective of the particular boron precursor

Table 3
MPV reduction of cinnamaldehyde by hydrogen transfer from 2-propanol. Products distribution, initial reaction rate and selectivity to cinnamyl alcohol obtained.

Catalyst	Products distribution (mol/L)				rg (mol/min g)10^6	rm^2 (mol/min m^2)10^9	%Conv	$\%S_{UOL}$
	C_{SAL}	C_{SOL}	C_{UAL}	C_{UOL}				
Zr–O	0.004	0.003	0.418	0.075	8.0	46.8	16.5[a]	88.2[a]
Zr–P	0.005	0.000	0.457	0.038	2.8	20.0	8.5[a]	87.8[a]
ZrB–OA	0.002	0.000	0.460	0.037	2.8	20.7	7.9[a]	94.5[a]
ZrB–OT	0.002	0.000	0.443	0.055	4.0	23.5	11.4[a]	97.0[a]
ZrB–PA	0.007	0.002	0.413	0.078	12.0	48.6	17.4[a]	88.3[a]
ZrB–PT	0.006	0.001	0.376	0.117	24.0	100.0	24.8[a]	92.9[a]
ZrMg–PN	0.002	0.000	0.425	0.074	1.7	9.9	8.3[b]–14.5[c]	97.4[c]
ZrCa–PN	0.002	0.001	0.386	0.111	3.0	19.4	12.8[b]–22.0[c]	97.5[c]
ZrSr–PN	0.002	0.001	0.378	0.120	3.8	19.8	14.2[b]–24.4[c]	98.1[c]
ZrBa–PN	0.002	0.000	0.407	0.091	2.0	9.5	11.2[b]–18.5[c]	97.8[c]

[a] Catalyst weight, 0.5 g: Reaction time, 8 h.
[b] Catalyst weight, 1.0 g: Reaction time, 8 h.
[c] Catalyst weight, 1.0 g: Reaction time, 24 h.

used, the catalysts in this series prepared from zirconium oxychloride (ZrB–O*) were more selective – and less active – than those obtained from zirconium propoxide (ZrB–P*).

In the previous work [46], we used thermal programmed adsorption/desorption of acrolein and DRIFT spectroscopy of the same compound adsorbed onto catalysts with variable acid–base properties to demonstrate that adsorption of the α,β-unsaturated compound on the catalyst was crucial with a view to ensure its selective reduction. Thus, the presence of basic sites in the solid ($MgO–B_2O_3$) facilitated interaction of the carbonyl group with the catalyst surface, thereby enabling selective reduction to the corresponding unsaturated alcohol [46]. With primarily acid catalysts ($SiO_2–AlPO_4$), however, acrolein was adsorbed via its C=C double bond, which detracted from the selectivity towards allyl alcohol [8,46]. It therefore seems clear that modifying ZrO_2 with an alkaline-earth metal enhances its basic properties and results in increased selectivity towards the unsaturated alcohol.

3.2.2. Influence of the catalyst synthetic procedure

Although the influence of the synthetic procedure and composition of the catalyst conformed to no definite pattern, modifying ZrO_2 with boron seemingly increased the initial catalytic activity, especially in the solids obtained from zirconium propoxide (ZrB–P*). In any case, the pure zirconium oxides were quite active (particularly that obtained from zirconium chloride, Zr–O). Finally, modifying ZrO_2 with an alkaline-earth metal detracted from its catalytic activity, particularly in ZrMg–PN and ZrBa–PN.

It is interesting to note that, although then initial reaction rate was expressed in term of catalyst surface, an additional relationship appeared to exist within each catalyst family (*viz.* pure zirconium oxides, boron-doped and alkaline-earth modified solids) between catalytic activity and specific surface area. As noted earlier, the specific surface area is ultimately related in a direct manner to crystallinity in the final solid: the higher the crystallinity, the lower is the S_{BET}. It therefore seems reasonable to assume that the catalytic activity in the process is somehow related to the catalyst crystallinity as exposed by its crystallization temperature, T_{glow}, determined from the TGA–DTA tests. Thus, the boron-doped catalysts exhibited a high correlation between the initial reduction rate and the glow exotherm temperature, T_{glow}: the higher was the temperature the lower was the crystallinity – and the higher the catalytic activity as a result. As stated above, the ZrB catalysts prepared from zirconium propoxide (ZrB–PA and ZrB–PT) exhibited better catalytic properties than those obtained from zirconium oxychloride (ZrB–OA and ZrB–OT). These differences can be ascribed to the amorphous nature of the ZrB–P* solids and the more crystalline (tetragonal) structure of the ZrB–O* solids (see Table 1).

Similar conclusions can be drawn for the series encompassing the pure zirconium oxides and those modified with an alkaline-earth metal. By exception, ZrBa–PN, which crystallized at a high temperature (T_{glow} = 590 °C) and was quite amorphous judging from its XRD pattern, exhibited the lowest initial catalytic activity in its series. However, as shown below, this may have been the result of the surface acid–base properties of the solids.

3.2.3. Influence of the catalyst surface acid–base properties

Properly understanding the way the degree of crystallinity of the catalyst can influence its activity in the MPV reaction requires careful analysis of the structural properties and, specifically, the surface–chemical characteristics of the solids.

The influence of surface acid sites on the catalytic activity is illustrated in Table 3, which shows the relationship between the total acidity per square metre of catalyst and the initial rate of cinnamaldehyde reduction. Also, Fig. 8 illustrates the relationship between the catalytic activity and the percent distribution of the different types of acid sites (*viz.* those interacting with pyridine via hydrogen bonding, Bronsted or Lewis type interactions) in each catalyst.

The results suggest that an increased density of acid sites leads to a decreased catalytic activity. Fig. 8 supports this statement. Thus, the catalysts containing largely weak acid sites, which interact with pyridine via hydrogen bonds, are the least active in the process. Such catalysts are the zirconium oxides modified with an alkaline-earth metal (essentially ZrCa–PN, ZrSr–PN and ZrBa–PN). By contrast, the most active solids are those containing the highest proportions of proton acid sites of medium–high strength, which establish Bronsted-type interactions with pyridine and include the pure and boron-modified zirconium oxides. Other

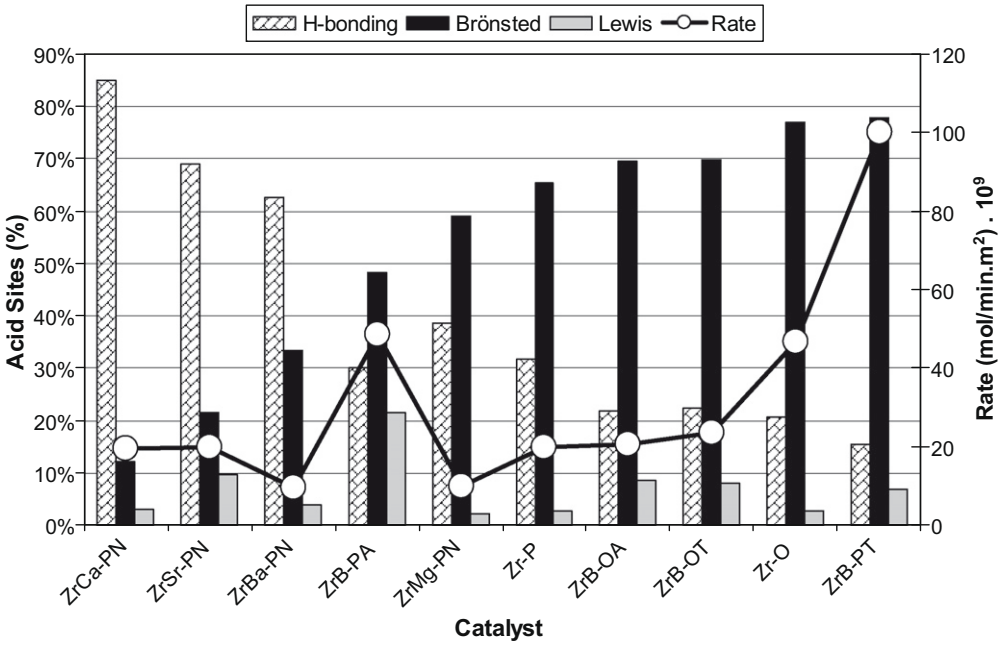

Fig. 8. Comparison between the catalytic activity (reaction rate) and the percent distribution of acid site types in each catalyst.

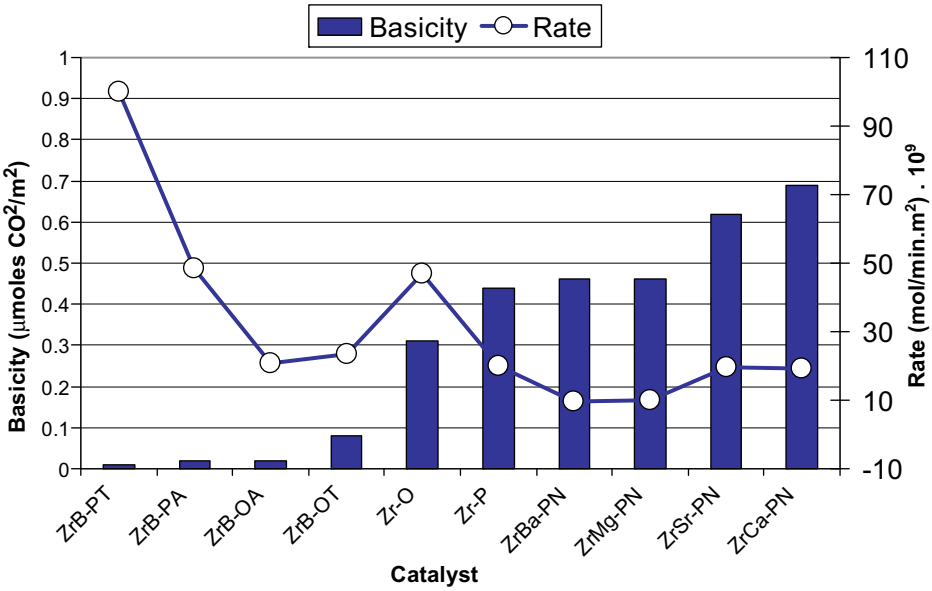

Fig. 9. Comparison between the catalytic activity (reaction rate) and the surface base properties of each catalyst.

authors [10,11] previously obtained similar results suggesting that Bronsted acid sites (hydroxyl groups) are very important in the studied process since hydroxyl groups facilitate exchange of the ligand with 2-propanol. The most salient exception to this rule was ZrB–PA, which exhibited a rather high initial catalytic activity – the second highest – despite containing a medium–low proportion of Bronsted acid sites. However, this catalyst also contained a very high proportion of Lewis acid sites (22%) relative to the others (2–10%), which may provide a plausible explanation for its abnormal behaviour.

Regarding surface basic sites, the most active catalysts in the process were those containing them in the lowest proportions (*viz.* those in the ZrB series, Fig. 9). Accordingly, the alkaline-earth-doped solids were the least active as they contained basic sites at higher densities.

It seems obvious that, if as noted by Liu et al. [11], the catalytically active sites in the process are proton (Bronsted) sites of medium–high strength, the solids containing the highest proportions of weak acid sites hydrogen-bonding to pyridine and/or basic sites at a high density should have been much less active in the MPV reduction of cinnamaldehyde. In any case, a potential contribution of Lewis acid sites cannot be ruled out since the only solid containing a substantial proportion of such sites, ZrB–PA, exhibited a moderately high catalytic activity. In this respect, some authors previously found Lewis acid sites to be involved in the MPV reaction [3,4].

The catalyst synthetic procedure and the way it is modified (by doping with boron or an alkaline-earth metal) affect the presence of surface hydroxyl groups in the solid and hence its catalytic activity. In fact, as stated above, the higher the catalyst crystallization temperature as measured by T_{glow}, the higher was its catalytic activity. Since a high T_{glow} value is indicative of an amorphous nature – all solids were calcined at 400 °C – the amorphous catalysts should contain an increased amount of surface hydroxyl sites. However, calcining at 400 °C the catalysts with a relative low T_{glow} value led ZrO_2 to crystallize in the tetragonal system and the number of surface hydroxyl groups in it – and its catalytic activity – to decrease as a result. This effect is therefore similar to that previously observed by Liu et al. in raising the calcination temperature of zirconium oxide over the range 200–500 °C [11].

In this respect, modifying ZrO_2 with boron or an alkaline-earth metal reduced its crystallinity and led to more amorphous catalysts. Unlike the alkaline-earth metals, however, the addition of boron gave more active catalysts. The origin of the increased activity is an increased proportion of essentially Bronsted sites resulting from the incorporation of B_2O_3 into the solid, as previously found by our group in other boron-modified catalytic systems [42,47,48]. On the other hand, the incorporation of an alkaline-earth metal gave solids with very weak acid sites interacting with pyridine via hydrogen bonds alone; such solids possessed fewer Bronsted acid sites and more basic sites, and were the least active among those studied.

These findings would complement results of other authors suggesting that the process takes place via Lewis acid sites in zeolites [3], basic sites in MgO [17] and basic zeolites [18] and acid–base pairs in calcined Mg and Al hydrotalcites [49]. In any case, the type of catalyst used appears to have a strong effect on the outcome of the process, which is also seemingly influenced by its synthetic procedure and thermal treatment, however.

4. Conclusions

Zirconium oxide catalysts are active in the chemoselective reduction of cinnamaldehyde by hydrogen transfer from an alcohol, which constitutes the Meerwein–Ponndorf–Verley (MPV) reaction. However, their activity and selectivity in the process vary markedly depending on the particular synthetic procedure and also on any modifications used to alter their acid-base properties.

The catalyst synthetic procedure and modifications used in this work (doping with boron or an alkaline-earth metal) were found to affect surface hydroxyl groups – and catalytic activity as a result. In fact, the higher the crystallization temperature (*i.e.* the *glow exotherm*, T_{glow}) of the catalyst, the higher was its activity. Since an increased T_{glow} value led to a poorly crystalline solid – all studied here were calcined at 400 °C – the amorphous catalysts contained an increased amount of surface hydroxyl sites. By contrast, calcination at 400 °C of the catalysts with a relatively low T_{glow} value caused ZrO_2 to crystallize in the tetragonal system and reduced the amount of surface hydroxyl groups, and hence their activity.

Proton (Bronsted) acid sites of medium–high strength are seemingly the most catalytically active; in fact, the solids with an increased proportion of weak acid sites (those hydrogen bonded to pyridine) and a high density of basic sites were much less active in the MPV reduction of cinnamaldehyde. In this respect, the

incorporation of boron into ZrO_2 leads to an increased catalytic activity consistent with the increased amount of highly strong proton (Bronsted) acid sites; the increased activity, however, was associated to a slight loss of selectivity towards cinnamyl alcohol, which fell down to 88%. Such a loss was a result of preferential adsorption of the substrate via its C=C double bond.

Modifying ZrO_2 with an alkaline-earth metal boosts its basicity, thereby leading to a decreased catalytic activity and an increased selectivity towards the unsaturated alcohol by effect of the α,β-unsaturated carbonyl compound being adsorbed in the optimal configuration for the MPV process.

Acknowledgments

The authors wish to acknowledge the financial support from the Consejería de Educación y Ciencia of the Junta de Andalucía (Projects FQM-191 and P07-FQM-02695) and the Spanish Ministerio de Educación y Ciencia (Projects CTQ2007-65754/PPQ, CTQ2008-01330/BQU, co-financed with FEDER funds). The authors are also grateful to Dr. I.M. García of the Central Research Support Service (SCAI) of the University of Córdoba for recording the ICP–MS spectra.

Appendix A. Supplementary material

Supplementary data associated with this article can be found, in the online version, at doi:10.1016/j.jcat.2009.09.005.

References

[1] V. Ponec, Appl. Catal. A 149 (1997) 27.
[2] P. Gallezot, B. Blanc, D. Barthomeuf, M.I. Pais da Silva, Stud. Surf. Sci. Catal. 84 (1994) 1433.
[3] E.J. Creyghton, R.S. Downing, J. Mol. Catal. A 134 (1998) 47.
[4] G.K. Chuah, S. Jaenicke, Y.Z. Zhu, S.H. Liu, Curr. Org. Chem. 10 (2006) 1639.
[5] A. Corma, S. Iborra, Adv. Catal. 49 (2006) 239.
[6] P.S. Kumbhar, J. Sanchez-Valente, J. Lopez, F. Figueras, Chem. Commun. (1998) 535.
[7] F. Braun, J.I. Di Cosimo, Catal. Today 116 (2006) 206.
[8] J.I. Di Cosimo, A. Acosta, C.R. Apesteguia, J. Mol. Catal. A 222 (2004) 87.
[9] J.I. Di Cosimo, A. Acosta, C.R. Apesteguia, J. Mol. Catal. A 234 (2005) 111.
[10] Y. Zhu, S. Liu, S. Jaenicke, G. Chuah, Catal. Today 97 (2004) 249.
[11] S.H. Liu, S. Jaenicke, G.K. Chuah, J. Catal. 206 (2002) 321.
[12] Y. Zhu, G.K. Chuah, S. Jaenicke, J. Catal. 241 (2006) 25.
[13] A. Ramanathan, D. Klomp, J.A. Peters, U. Hanefeld, J. Mol. Catal. A 260 (2006) 62.
[14] A. Ramanathan, M.C. Castro Villalobos, C. Wakernaak, S. Telalovic, U. Hanefeld, Chem. Eur. J. 14 (2008) 961.
[15] S. Nishiyama, M. Yamamoto, H. Izumida, S. Tsuyura, J. Chem. Eng. Jpn. 37 (2004) 310.
[16] V. Ivanov, J. Bachelier, F. Audry, J.C. Lavalley, J. Mol. Catal. 91 (1994) 45.
[17] M. Berkani, J.L. Lemberton, M. Marczewski, G. Perot, Catal. Lett. 31 (1995) 405.
[18] J. Lopez, J.S. Valente, J.-M. Clacens, F. Figueras, J. Catal. 208 (2002) 30.
[19] G. Szollosi, M. Bartok, J. Mol. Struct. 482–483 (1999) 13.
[20] G. Szollosi, M. Bartok, Appl. Catal. A 169 (1998) 263.
[21] G. Szollosi, M. Bartok, J. Mol. Catal. A 148 (1999) 265.
[22] K. Tanabe, T. Yamaguchi, Catal. Today 20 (1994) 185.
[23] C.J. Zhang, R. Miranda, B.H. Davis, Catal. Lett. 29 (1994) 349.
[24] F. Lonyi, J. Valyon, J. Therm. Anal. 46 (1996) 211.
[25] K. Arata, Appl. Catal. A 146 (1996) 3.
[26] D. Spielbauer, G.A.H. Mekhemer, T. Riemer, M.I. Zaki, H. Knozinger, J. Phys. Chem. B 101 (1997) 4681.
[27] U. Usman, M. Takaki, T. Kubota, Y. Okamoto, Appl. Catal. A 286 (2005) 148.
[28] F.M. Bautista, J.M. Campelo, A. Garcia, D. Luna, J.M. Marinas, M.C. Moreno, A.A. Romero, Appl. Catal. A 170 (1998) 159.
[29] D. Mao, G. Lu, Q. Chen, Appl. Catal. A 279 (2005) 145.
[30] K.M. Malshe, P.T. Patil, S.B. Umbarkar, M.K. Dongare, J. Mol. Catal. A 212 (2004) 337.
[31] B.Q. Xu, S.B. Cheng, X. Zhang, Q.M. Zhu, Catal. Today 63 (2000) 275.
[32] M.A. Aramendia, V. Borau, C. Jimenez, J.M. Marinas, A. Porras, F.J. Urbano, J. Mater. Chem. 9 (1999) 819.
[33] M. De, D. Kunzru, Catal. Lett. 102 (2005) 237.
[34] C. Flego, G. Cosentino, M. Tagliabue, Appl. Catal. A 270 (2004) 113.
[35] J.I. Dicosimo, V.K. Diez, C.R. Apesteguia, Appl. Catal. A 137 (1996) 149.
[36] J. Trawczynski, J. Walendziewski, Appl. Catal. A 119 (1994) 59.
[37] H. Wang, M. Wang, N. Zhao, W. Wei, Y. Sun, Catal. Lett. 105 (2005) 253.
[38] S. Brunauer, P.H. Emmett, E.J. Teller, J. Am. Chem. Soc. 60 (1938) 309.
[39] E.P. Barrett, L.S. Joyner, P.P. Halenda, J. Am. Chem. Soc. 73 (1951) 373.
[40] A.A.M. Ali, M.I. Zaki, Colloid Surf. A 139 (1998) 81.
[41] R. Burch, C. Passingham, G.M. Warnes, D.J. Rawlence, Spectrochim. Acta A 46 (1990) 243.
[42] M.A. Aramendia, V. Borau, C. Jimenez, J.M. Marinas, J.R. Ruiz, F.J. Urbano, J. Colloid Interf. Sci. 217 (1999) 186.
[43] P.J. Hendra, J.R. Horder, E.J. Loader, J. Chem. Soc. (1971) 1766.
[44] P.J. Hendra, I.D.M. Turner, E.J. Loader, M. Stacy, J. Phys. Chem. 78 (1974) 300.
[45] M.I. Zaki, A.A.M. Ali, Colloid Surf. A 119 (1996) 39.
[46] M.A. Aramendia, V. Borau, C. Jimenez, A. Marinas, J.M. Marinas, A. Porras, F.J. Urbano, Catal. Lett. 50 (1998) 173.
[47] M.A. Aramendia, V. Borau, C. Jimenez, J.M. Marinas, A. Porras, F.J. Urbano, J. Catal. 161 (1996) 829.
[48] M.A. Aramendia, V. Borau, C. Jimenez, J.M. Marinas, A. Porras, F.J. Urbano, J. Mater. Chem. 6 (1996) 1943.
[49] T.M. Jyothi, T. Raja, B.S. Rao, J. Mol. Catal. A 168 (2001) 187.